Correlation and evolution of the blazar S5 1803+784 short-term variability properties during 01.2022–01.2023

M. Butuzova, M. Gorbachev, V. Guseva, A. Zhovtan, S. Nazarov, G. Baida, and A. Krivenko

Crimean Astrophysical Observatory of the Russian Academy of Sciences, Nauchny, 298409 Russia

Abstract. The blazar S5 1803+784 has a unique high temporal resolution data series for about a year provided by the TESS satellite. By performing our aperture photometry of summarized on 10–30 the full-frame image cuts to reduce Poisson noise, we obtained the blazar light curve from 01.2022 to 01.2023. Using a new method for determining the shortest characteristic variability time and supplementing the study with data from long-term multiband ZTF and AZT-8 observations, we trace the evolution of the micro-variability parameters and their correlation to the long-term variability characteristics. We draw a conclusion regarding the mechanism, forming the S5 1803+784 micro-variability.

1 Introduction

The predominant part of the observed blazar radiation is formed in their ultra-relativistic jets and is characterized by strong variability in the entire observable electromagnetic spectrum. The study of optical radiation is of interest because it comes from a region located in extreme proximity to the place of collimation and acceleration of matter in the jet. In the optical range, studies of intra-day variability are important for determining the variability mechanisms, and, as a consequence, the structure of jet flow (see, for example, Marscher 2014; Butuzova 2021).

At the same time, the duration of the data series is limited due to the Earth's daily rotation and weather conditions. The situation has been changed by space observatories specialized in searching for exoplanets. Namely, the Kepler satellite obtained the 181-day light curve of BL Lac object W2R 1926+42 (Edelson et al. 2013). For blazars S5 0716+714 (Raiteri et al. 2021a) and S4 0954+65(Raiteri et al. 2021b), characteristic variability times exceeding one day were identified based on TESS data for one or more sectors. The study of the temporal variability characteristics on time scales of several days requires a statistically significant data set and, consequently, the duration of a (quasi)uniform series of observations over at least several sets of TESS. Such a data series can be obtained for blazars located near the ecliptic poles, which TESS monitors during 13 sets interchangeably.

2 Light curve and spectral index of S5 1803+784

The TESS observations of blazar S5 1803+784 cover sectors 47–55 and 56–60 (entire period is 01.01.2021–18.01.2023). The light curves obtained by the standard algorithms for extracting SAP and PDCSAP fluxes are not applicable in our case because they are highly susceptible to Poisson noise due to the low brightness of the object and the small number of pixels containing the image of the object (Butuzova et al. 2024). We obtained the S5 1803+784 light curve by aperture photometry summed up by ten TESS full-frame image cuts for the object and comparison stars (Fig. 1). Depending on the object brightness and the TESS frame exposure, the time resolution of the data studied ranged from 67 to 300 minutes. Figure 2 shows the obtained light curves of the blazar S5 1803+784 and the control star, supplemented by photometric observations of ZTF (band r) and AZT-8 (band R of the Johnson system). There is a good correspondence between the light curves, except for the period of low brightness of the object. We believe that the difference in the variability amplitude in sectors 47, 51, 58–60 arises because the blazar's brightness has become the same or less than the brightness of the neighboring star and, consequently, the contribution of the latter's radiation to the aperture has increased and become significant.
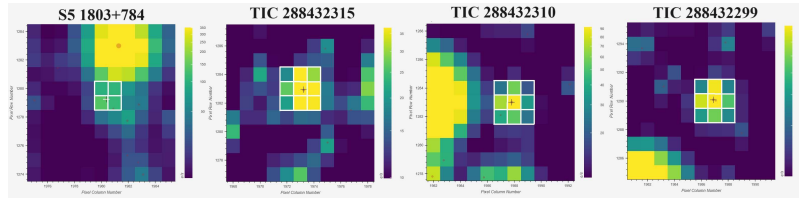
Fig. 1. TESS full-frame image cuts of S5 1803+784 and comparison stars for 53 sectors. The cross denotes the position of the specified objects. The white border marks the pixels of the aperture.
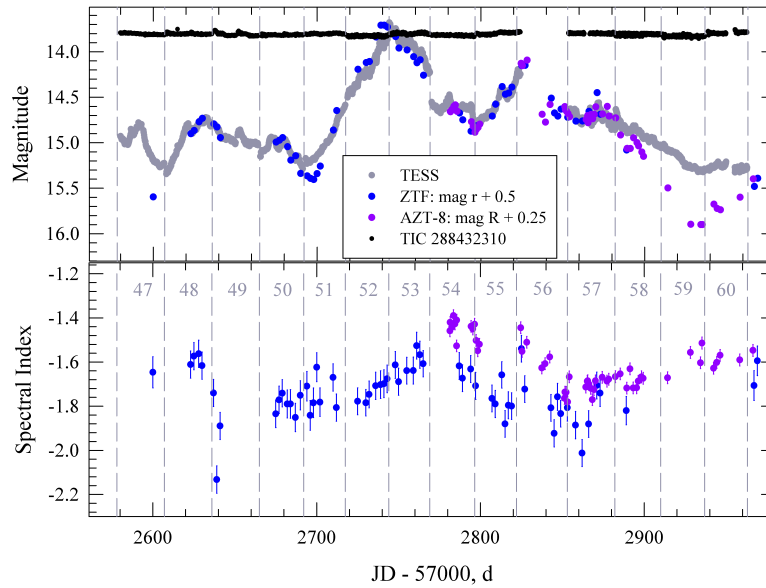

Fig. 2. The light curve of S5 1803+784 (top) and the evolution of the spectral index (bottom) from 01.01.2021 to 18.01.2023 according to TESS, ZTF, and AZT-8 data. Vertical dashed lines mark the boundaries of the TESS sectors, the number of which is shown in gray.

We determined the spectral index α ($F \propto \nu^{\alpha}$) from quasi-simultaneous observations in two or more bands. The errors of the α values were estimated according to the method described by Gorbachev et al. (2024). The spectral index varied from -1.4 to -2.2, not correlating with changes in brightness (Fig. 2, bottom panel).

3   Temporal parameters of variability

The high-time resolution light curve S5 1803+784 (Fig. 2) can be characterized as a superposition of variations occurring on different time scales. Taking into account the measurement accuracy, it is natural to assume that there is some minimum characteristic variability time τ, the value of which can evolve. We assume that in the radiating region, at each moment, there is one dominant process leading to the observed micro-variability, which then changes its parameters or is replaced by another one, having a different τ. Determining the characteristic variability time, for example, by the structure function (SF, Simonetti et al. 1985), when using a light curve containing the results of several such short-term processes, is incorrect. It is because, on a short time scale, processes with different τ neutralize each other's manifestation, and the type of structural function will be influenced by a process operating on a longer time scale.
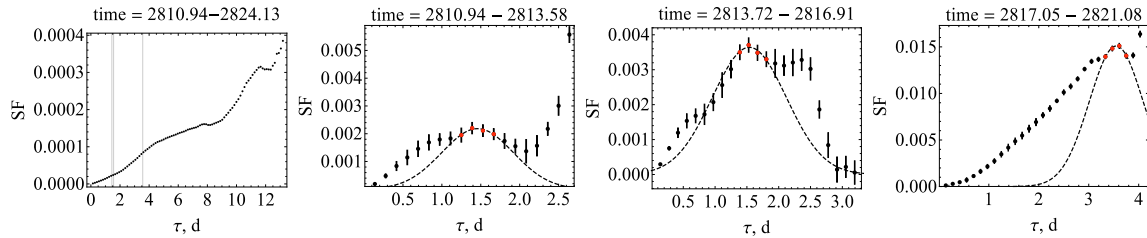

Fig. 3. SF for continuous light curve part of 55th sector (left) and SFs for small time interval within it. Vertical lines mark found τs.

To determine the shortest τ, we divided the TESS light curve of S5 1803+784 into parts within which no more than one point was allowed to be consecutive omitted in a uniform data series and acted according to the algorithm described by Butuzova et al. (2024). Namely, for each of these parts, an initial interval limited to twenty points was taken, and the SF was calculated. This interval was increased until τ, defined as the position of the SF peak, was found. Then we moved on to the next 20-point interval and performed the described algorithm. Figure 3 shows an example of the result of interval separation on the light curve characterized by different τ.

It can be seen that the found τ does not appear on the SF, constructed from all the data, the initially selected part of the light curve. The evolution of the mean magnitude, τ, and the square of the mean variability amplitude SF_{max} (defined as the value of the SF peak) are shown in Fig. 4.
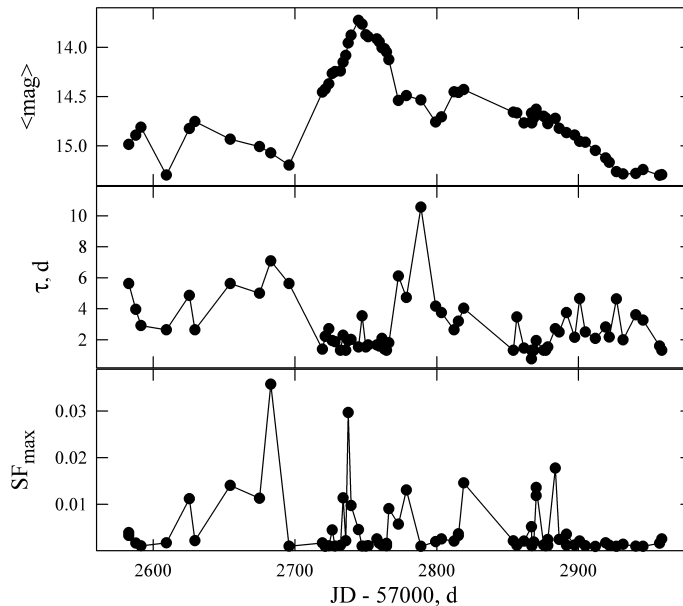

Fig. 4. The evolution of the average magnitude, characteristic variability time, and the square of the average amplitude of the micro-variability (from top to bottom).

4   Results

Due to the absence of the $SF_{max}(\tau)$ correlation (Fig. 5), it follows that there is the action of either several micro-variability mechanisms or one determined by two or more independent parameters. These parameters do not depend on the characteristics of long-term variability, such as the average brightness <mag> and the maximum brightness change Δmag in the intervals corresponding to the found characteristic variability times.

We believe that the natural explanation for the observed properties of micro-variability is as follows. Regardless of the parameters and mechanisms of long–term
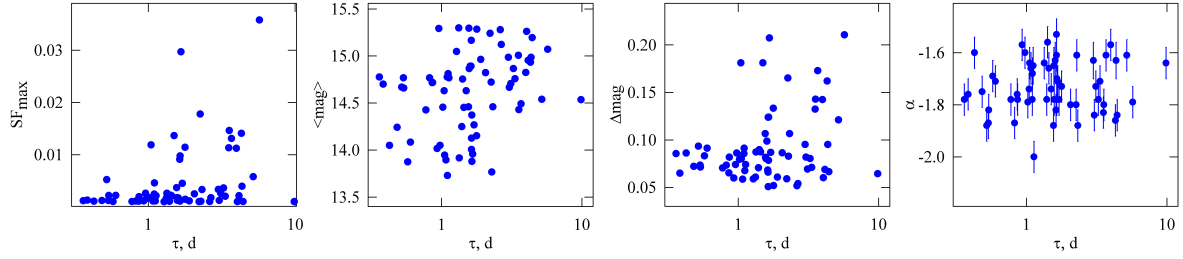
Fig. 5. Dependencies of the micro-variability parameters (SF_{max}, $<mag>$, Δmag) and the spectral index on τ.

variability, there are sub-components in the jet flow, which are parts of the emitting region, having motion direction differing slightly (within a few degrees) from the main trajectory. It leads to the fact that the sub-components have a Doppler factor that differs from the Doppler factor of the main flow, which results in micro-variability events. In this case, the absence of $SF_{max}(\tau)$ dependence indicates that the sub-components have different volumes. Further detailed modeling of the sub-components with different relations between their volume and the Doppler factor will allow us to draw conclusions about the structure of the jet flow.

References

Butuzova M., 2021, Astroparticle Physics, 129, id. 102577

Butuzova M., Guseva V., Gorbachev M., Krivenko A., and Nazarov S., 2024, in prep.

Edelson R., Mushotzky R., Vaughan S., et al., 2013, Astrophys. J., 766, p. 16

Gorbachev M., Butuzova M., Nazarov S., and Zhovtan A., 2024, Astroparticle Physics, 160, id. 102965

Marscher A., 2014, Astrophys. J., 780, p. 87

Raiteri C., Villata M., Carosati D., et al., 2021a, Monthly Not. Roy. Astron. Soc., 501, p. 1100

Raiteri C., Villata M., Larionov V., et al., 2021b, Monthly Not. Roy. Astron. Soc., 504, p. 5629

Simonetti J., Cordes J., and Heeschen D., 1985, Astrophys. J., 296, p. 46